Effect of Annealing Process on the Heteroepitaxial Cuo/Cu2O as a Highly Efficient Photocathode for Photoelectrochemical Solar Cell Application

M. Abdurrahman

Department of Physics, Faculty of Physical Science, Federal University, Dutse, Nigeria

*Corresponding author; Email: Msabdurrahaman@yahoo.com

Article Info

Article history:

Received , 18/10/2025
Revised , 16/11/2025
Accepted , 12/12/2025

Keywords:

Heteroepitaxial;
Solar cell;
Photocathode;
Photoanode;
Photocurrent.

ABSTRACT

The thermal oxidations of cuprous oxide were effectively prepared via simply annealing on copper foil substrate Cu_2O photocathodes. They were characterized by Fourier transport infrared spectroscopy (FTIR), scanning electron microscopy (SEM). The results during the annealing process showed that a heteroepitaxial layer of CuO/Cu_2O formed, which displayed the nature of a p-type semiconductor. Compared to pure Cu_2O, the photocurrent density and photoelectrochemical (PEC) stability of the p-type heteroepitaxial CuO/Cu_2O photocathode improved significantly, largely due to changes in annealing time and temperature. The best performance and stability were achieved by annealing at 475°C, showing a considerable enhancement over the as-deposited Cu_2O. This indicates that the CuO/Cu_2O heteroepitaxial layer helps separate electron-hole pairs, boosting both the current and stability of the photocathode. Although the heteroepitaxial layer is thin, its effect on catalytic activity is substantial. It alters the band and electronic structures of $Cu\text{-}Cu_2O$, which aids in activating O_2 and transferring electrons during the oxidation process, thereby enhancing catalysis.

I. Introduction

Recently, there has been a lot of interest in semiconductor photocatalysis because it can help produce hydrogen and remove pollutants. These are important ways to address both energy and environmental issues [1–7]. Compared to the traditional photocatalytic process, using a photoelectrochemical (PEC) cell makes it easier to separate products and production of electricity [5]. An ideal PEC system would need a photoanode (n-type semiconductor) for oxidation and/or a photocathode (p-type semiconductor) for reduction [6]. Titanium dioxide (TiO_2), an n-type semiconductor, is widely used for treating pollutants [8,9]. While many studies focus on creating efficient n-type semiconductor photoanodes, there are fewer reports about effective photocathodes. Most PEC systems use platinum as the cathode for reduction of water, but this raises the cost of the PEC system. Therefore, it is interesting to look for new cathode materials that are cheaper and made from more readily available resources instead of platinum. For many oxide-based photocathodes, such as $CaFe_2O_4$, $SrTiO_3$, $CuFe_2O_4$, $LaFeO_3$ and $ZnFe_2O_4$ [10–14], face challenges like availability, cost, and complex production methods limit their use. On the other hand, cuprous oxide (Cu_2O) prove that is a promising candidate because it is easy to prepare, abundant in nature, non-toxic, naturally p-type, and can absorb visible light with a direct band gap of 2.0 eV[15,16]. The poor stability of the photo in water-based electrolytes and the quick recombination of charge carriers significantly hinder the practical use of Cu_2O in photoelectrochemical (PEC) applications.

To address these issues with Cu_2O, researchers have looked into several effective methods. For example, studies have shown that creating heterostructures through layer-by-layer deposition of n-type semiconductors with more positive conductive bands, such as ZnO, TiO_2, and CdO, can improve photo corrosion resistance and stability [17–21]. There are several reports of making P-Cu_2O/n-Cu_2O and n-Cu_2O/pCu_2O using a two-step electro-deposition method, but this approach is complicated and results in unstable samples [22,23]. Additionally, the CuO/Cu_2O heterojunction synthesized by heating deposited copper on FTO exhibited high dark current, low photo current, poor photo stability and was prone to detaching from its substrate [24]. It is known that the conduction band minimum (CBM) of Cu_2O is slightly higher than that of CuO, while the valence band maximum (VBM) of CuO is lower than that of Cu_2O [25,26]. The differing band edges within the CuO/Cu_2O heterojunction may help in separating electrons and holes effectively [27,28]. Among various p-type semiconductors, cuprous oxide (Cu_2O), which has a direct band gap of 2.0 eV, shows promise as a photocathode material [29-32]. In this study, we introduce a simple method for synthesizing Cu_2O/CuO on a copper substrate. We synthesized the CuO/Cu_2O heteroepitaxial structure in two steps by oxidizing a copper film into cuprous oxide (Cu_2O). With an optimal ratio of CuO to Cu_2O, our sample synthesized at 475°C showed the best performance according to photoelectrochemical solar cell tests. This process is straightforward, easy to scale up, does not require templates, is inexpensive, and environmentally friendly. We thoroughly examined how annealing time affects crystallinity, morphology, structure, and photoelectric properties.

II. Research Method

We cut copper foil into squares measuring 2cm x 2cm. Subsequent we cleaned the pieces using ultrasonic waves with 2 proponal, ethanol and distilled water. After that, we preheated the substrates in a microwave oven at 250°C for 10 minutes to eliminate any leftover water and unwanted solvents on their surfaces. We then placed them in a clean envelope while waiting for the oxidation temperature to be reached. The samples were positioned between ceramic crucibles and placed in a high-temperature furnace set to 950℃, where they oxidized for 8 minutes. Immediately afterward, we quenched them in cold distilled water and dried them by placing them between tissue papers and finally letting them to air dry. The samples showed the structure displayed below (see Figure 1).

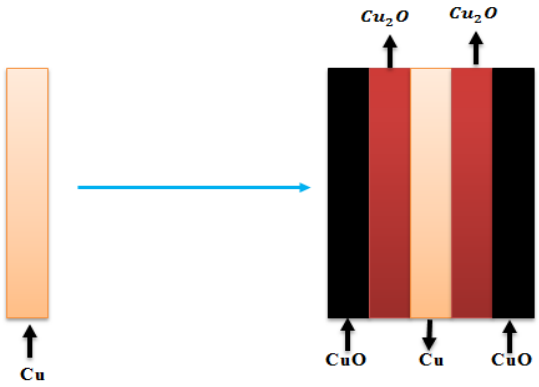

Figure 1. Block illustration of the engraving process

The thermal oxidized films were heated at various temperatures to heal appeared defects in the samples that occurred during the long oxidation process, which was done at temperatures of 460℃, 465℃, 470℃, 475℃, 480℃, 485℃, 490℃, and 495℃.

The pH of the electrolytic solution was kept constant by diluting NaCl as the PEC analysis electrolyte. The preparative parameters such as oxidation time, annealing time, weight of the as prepared sample and temperature were optimized by noting short circuit current (I_{sc}) and open circuit voltage (V_{oc}) of the PEC cell formed by the films deposited at various preparative parameters to get more photosensitive Cu_2O thin films.

The PEC cell was fabricated by using Cu_2O thin film as active photoelectrode, Sodium Chloride solution as an electrolyte and copper as a counter electrode and was illuminated under the solar irradiance as shown in figure 2.

The water compartment was inserted between the counter electrode and the main electrode to allow the direct heating of the cell. The films deposited at optimized preparative parameters were annealed at eight different temperatures. Annealing temperature was also optimized by PEC technique.

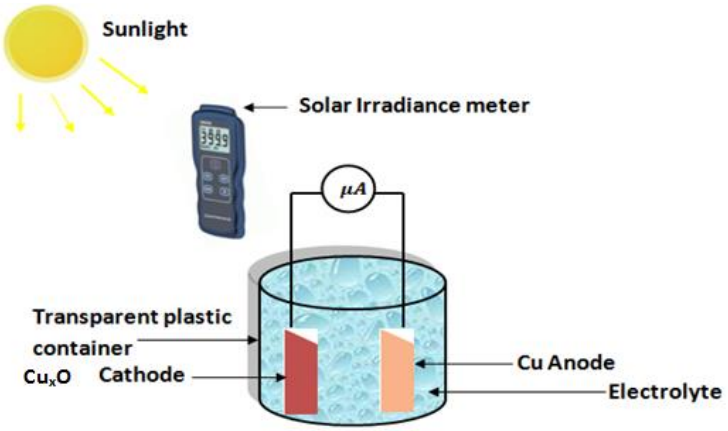

Figure 2. Illustration of the fabricated Cu – Cu_xO Photoelectrochemical solar cell.

III. Results and Discussion

III.1. Surface Morphology

Figure 2 shows SEM images of the films both as they were deposited and after being annealed at a temperature of 400 °C. The images indicate that the surface of the film became quite smooth after annealing, and no cracks appeared even though the O/Cu ratio increased significantly due to the annealing process.

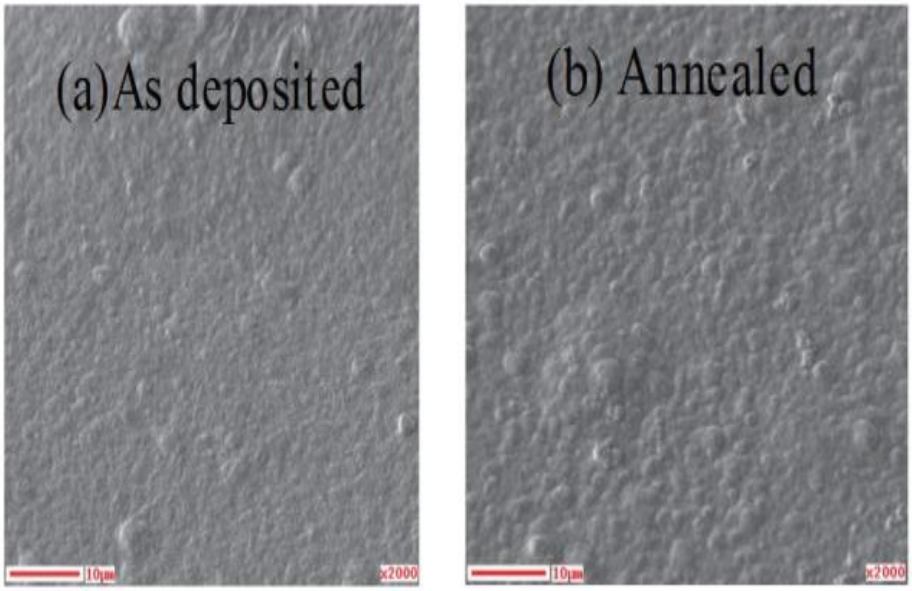

Figure 3. SEM photographs for the films of (a) as deposited and (b) annealed at 400°C.

Figure 3 displays the surface and cross-sectional views of both the as-deposited Cu_2O and the samples that were annealed at different temperatures. The findings indicate that the morphology of the samples changed noticeably

after annealing. The as-deposited Cu_2O appeared red-brown, featuring a compact pyramid-like structure with a thickness of 917 nm. However, after being annealed at 400°C (referred to as as-annealed-400°C), the surface transformed from pyramid-like shapes to irregular small particles, although some faint outlines of the original pyramids (marked by the highlighted red circle) were still visible.

III.2. Photoelectrochemical Solar Cell Performance

The PEC performances of both the newly deposited Cu_2O sample and the annealed photocathodes samples were examined using two-electrode setup under illumination [33]. The analyzed current-potential curves from eight different samples that were annealed at various temperatures (460°C, 465°C, 470°C, 475°C, 480°C, 485°C, 490°C, and 495°C), as well as an unannealed sample. All findings are illustrated in Figure 3, which highlights the PEC analysis of the most effective synthesized sample. The results revealed that the CuO/Cu_2O photocathode synthesized at 470°C produced a significantly higher photocurrent density compared to the Cu_2O photocathode and the other seven samples (460℃, 465℃, 475℃, 480℃, 485℃, 490℃ and 495℃) heated at different temperatures. The slope of the Mott-Schottky plot for those samples was negative, indicating that they acted as p-type semiconductors. To test stability of the synthesized sample under illuminated the photocathodes annealed at various temperatures were characterized for 10 minutes, with results shown in Figure 3. The photocurrent density of the sample heated to 470 °C was five times greater than that of the bare Cu_2O photocathode. This finding suggests that creating CuO/Cu_2O heteroepitaxial structures can enhance light absorption and improve charge carrier transport.

Table 1: The values of current-voltage charactreristic curve under illumination

I(mA)	54.0	0.0	50.0	53.4	53.1	45.0
V(mv)	0.0	96.0	83.0	89.3	93.2	94.5

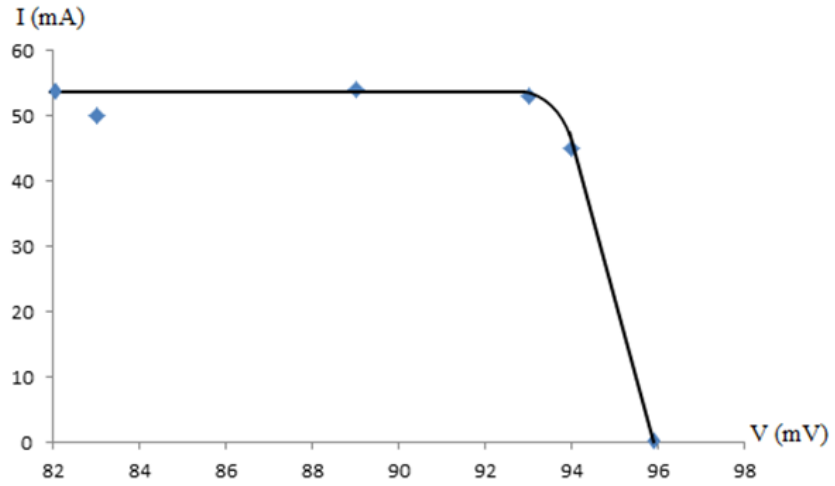

Figure 4. The graph of current – voltage characteristic of Cu-Cu_2O photoelectrochemical solar cell.

By observing the maximum values of I_{sc} and V_{oc} of the PEC cell the Optimization of preparative parameters is carried out. Figure 4 show the PEC analysis arrangement of the characteristic variation of I_{sc} and V_{oc} with deposition time. From the graph it is observed that I_{sc} and V_{oc} rises with increase in deposition time, attains maximum values for film deposited at 60 min and extra increase in deposition time both I_{sc} and V_{oc} decrease, this shows that the formation of good quality and practically stoichiometric compound at 60 min.

III.3. Fourier infrared spectroscopy (FTIR)

Figure 4 displays the FTIR analysis of annealed Cu_2O at temperatures of 460°C, 465°C, and 470°C. The results show that all samples have more than five peaks, except for the one at 465°C, which does not show a complete single peak. This suggests that the chemical being analyzed is complex because of the numerous peaks observed. Hydrogen bonds appear in a broad absorption band between 3650 and 3250 cm^{-1} [33]. The presence of hydroxyl

compounds is also confirmed by spectra found at frequencies ranging from 1600–1300, 1200–1000, and 800–600 cm^{-1}. A peak indicating that aromatic structures is present at 3088 cm^{-1}, which falls between 3000 and 3200 cm^{-1} [34]. Narrow bond peaks below 3000 cm^{-1} are attributed to C-C bonds. Additionally, a range of triple bonds from 2000 to 2500 cm-1 indicates the presence of C≡C bonds in the material [35,36]. In the double bond region (1500–2000 cm^{-1}), there is a prominent sharp peak that points to the existence of a double bond. This suggests that there might be a carbonyl double bond from ketones, aldehydes, esters, or carboxylic acids. All these peaks are present in both the samples at 460°C and 470°C. [34] Peaks in the single bond region can be seen between 2500 and 4000 cm^{-1}, with oxygen-related bonding indicated by a sharp bond around 3506 cm^{-1} that appears only in the sample annealed at 460°C. The peaks that show up only in the sample heated at 470°C were explained below. The sharp bond around 3506 cm^{-1} indicates that oxygen-related bonding is present. There are narrow bond peaks below 2920 cm^{-1}, which are linked to the OH bond. A peak near 1629 cm^{-1} shows the presence of C = C bonds in the sample. The peak at 1462 cm^{-1} signifies an aromatic ring. The band at 3320 cm^{-1} represents the NH_2 stretch. The peak at 2950 cm^{-1} corresponds to symmetric O-H vibration. Another peak at 1621 cm^{-1} indicates an O-H bond. The peak at 1439 cm^{-1} is due to C-H bending vibration, while the peak at 807 cm^{-1} represents C-N bonds in the samples. Lastly, a benzene ring is indicated by a peak at 1421 cm^{-1}. [36]

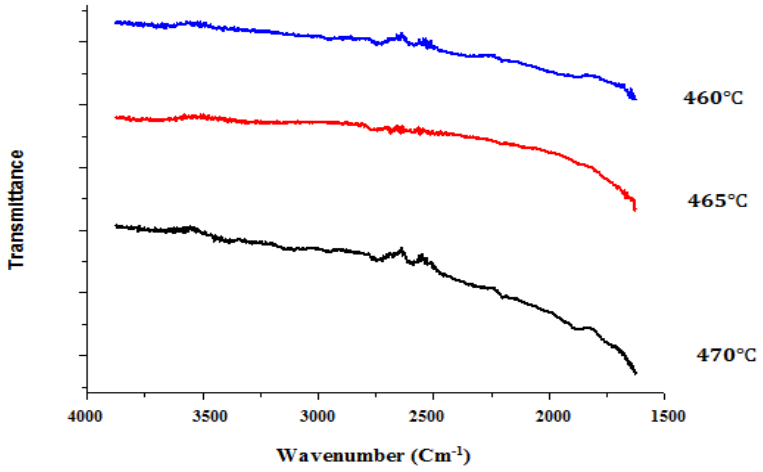

Figure 4. The analysis of the annealed Cu_2O FTIR at 460°C, 465°C and 470°C.

Figure 5 presents the analysis of the annealed Cu_2O FTIR at temperatures of 475°C, 480°C, and 485°C. In graph we found those hydrogen bonds in a broad absorption band between 3650 and 3250 cm^{-1} (Abdurrahman et al., 2023). In the graphs also confirmed the presence of hydroxyl compounds because of spectra observed at frequencies of 1600–1300, 1200–1000, and 800–600 cm^{-1}. The sharp bond around 3506 cm^{-1} indicates oxygen-related bonding. Aromatic structures are identified by a peak at 3088 cm^{-1}, which falls between 3000 and 3200 cm^{-1} (Abdurrahman et al., 2023). There are narrow bond peaks below 2920 cm^{-1} due to OH bonds. No distinct peak for aldehyde was detected in the range of 2700 to 2800 cm^{-1}. A range of triple bonds from 2000 to 2500 cm^{-1} suggests the presence of C≡C bonds in the material (Abdurrahman et al., 2023; Abdurrahman et al., 2023). A peak around 1629 cm^{-1} shows C = C bonds in the sample, while a peak at 1621 cm^{-1} represents O-H bonds. All these peaks are apparent at temperatures of 475°C, 480°C, and also at 485°C. Two similar peaks appear at both 475°C and 480°C one at 807 cm^{-1} representing C-N bonds in the samples and another at a peak of 1421 cm^{-1} related to the benzene ring. Three similar peaks point out at both 480°C and 485°C. These peaks, which indicate aromatic structures can be perceived with a peak at 3088 cm^{-1}, falling between 3000 and 3200 cm^{-1} (Abdurrahman et al., 2023). In the double bond region (1500-2000 cm^{-1}), there is a large, sharp peak that suggests a double bond's presence. Additionally, the band at 3327 cm^{-1} indicates the urethane-N-H stretch. At both 475°C and 485°C, two similar peaks appear: the band at 3320 cm^{-1} indicates the NH_2 stretch, while the peak at 2950 cm^{-1} corresponds to symmetric O-H vibration. At 475°C, two unique peaks are found the peak at 1462 cm^{-1} represents an aromatic ring, and the peak at 1439 cm^{-1} is due to C-H bending vibration. At 485°C, two distinct peaks also emerge: the peak at 1470 cm^{-1} signifies melamine-N-H, and the peak at 2325 cm^{-1} indicates P-H stretching.

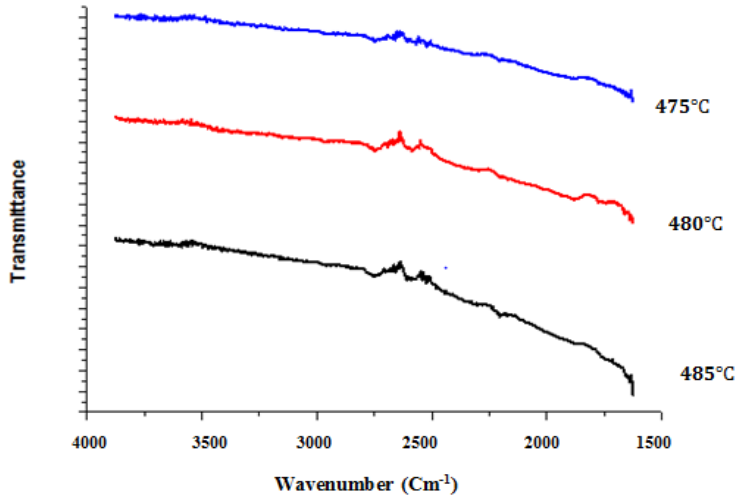

Figure 5. The analysis of the annealed Cu_2O FTIR at 475°C, 480°C and 485°C.

Figure 6 presents the analysis of the annealed Cu_2O FTIR at temperatures of 490°C and 495°C. The presence of more than five peaks suggests that the analyzed chemicals consist of complex molecules. Hydrogen bonds are detected in a broad absorption band between 3650 and 3250 cm^{-1} (Abdurrahman et al., 2023). Additionally, hydroxyl compounds are confirmed by the spectra seen at frequencies of 1600–1300, 1200–1000, and 800–600 cm^{-1}. Sharp bonding related to oxygen appears around 3506 cm^{-1}. A range of triple bonds from 2000 to 2500 cm^{-1} indicates the existence of C≡C bonds in the material (Abdurrahman et al., 2023; Abdurrahman et al., 2023). In the double bond region (1500-2000 cm^{-1}), a projecting peak signifies a double bond's presence, which could be due to carbonyl double bonds from ketones, aldehydes, esters, or carboxyl groups. The peak at 1439 cm^{-1} is associated with C-H bending vibrations. All these peaks are found in both samples at 490°C and 495°C. At 490°C, unique peaks in the single bond region occur between 2500 and 4000 cm^{-1}. Aromatic structures show a peak at 3088 cm^{-1} within the range of 3000 to 3200 cm^{-1} (Abdurrahman et al., 2023). Narrow bond peaks below 3000 cm^{-1} relate to C-C bonds. The band at 3320 cm^{-1} corresponds to NH_2 stretching, while the one at 2325 cm^{-1} represents P-H stretching. The distinct peak at 1629 cm^{-1} observed only at 490°C indicates the presence of C=C bonds in that sample.

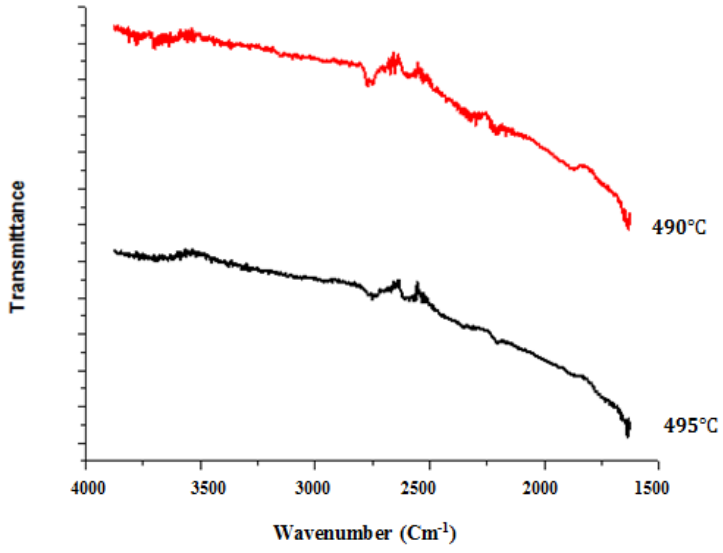

Figure 6. the analysis of the annealed Cu_2O FTIR at 490°C and 495°C.

IV. Conclusion

In summary, we have prepared a highly efficient and promising CuO/Cu_2O photocathode using a straightforward, affordable method. The preparation method comprised thermal oxidation and thermal annealing in air. Annealing treatment of the film in air shows an improvement in the polycrystalline nature of the film. The highest photo current density and stability were recorded on the CuO/Cu_2O heteroepitaxial annealed at 475°C for 15 min. To prepare good quality deposits, optimization of preparative parameters by PEC technique is suitable. As evidenced by characterization results, the improved photo electrochemical performance was attributed to the formation of the CuO/Cu_2O heteroepitaxial, which made the photogenerated electron-hole pairs effectively separated. The annealing process in air improved the film's polycrystalline quality. Both the as-deposited and annealed films showed nearly perfect compound formation. The optical and morphological, analysis of as-deposited as well as annealed films has been carried out. Annealing treatment of the film in air shows an enhancement in the polycrystalline nature of the film synthesized optimizing output of the PEC analysis. The as-deposited and annealed films showed nearly stoichiometric compound formation. By concocting a single orientation of CuO thin film poor mobility of an electron inside the oxide layer can be further enhanced. Higher grain size offers less barriers for electron mobility.

Acknowledgements

I would like to show gratitude Federal University Dutse and Tertiary Educational Fund, for providing favorable environment, equipment during the researchwork.

References

[1] Sun Z, Cao R.X, Huang M.H, Chen D.H., Zheng W., Lin L., (2015). Effect of light irradiation on the photoelectricity performance of microbial fuel cell with a copper oxide nanowire photocathode, J. Photochem. Photobiol. A 300 38–43.

[2] Hoffmann M.R., Martin S.T., Choi W., Bahnemann D.W., (1995). Environmental applications of semiconductor photocatalysis, Chem. Rev. 95 69–96.

[3] Li Y, Zhang J.Z, (2009). Hydrogen generation from photoelectrochemical water splitting based on nanomaterials, Laser Photonics Rev. 4 517–528.

[4] Chen X.B, Sheng S.H., Guo L.J, Mao S.S, (2010). Semiconductor-based Photocatalytic hydrogen generation, Chem. Rev. 110 6503–6570.

[5] Paracchino A, Laporte V., Sivula K., Gratzel M., Thimsen E., (2010). Highly active oxide photocathode for photoelectrochemical water reduction, Nat. Mater. 10 456–461.

[6] Abe R, (2010). Recent progress on photocatalytic and photoelectrochemical water splitting under visible light irradiation, J. Photochem. Photobiol. C 11 179–209.

[7] Mao C., Zuo F., Hou Y., Bu X., Feng P., (2014). In situ preparation of a Ti_3+ self-doped TiO_2 film with enhanced activity as photoanode by N_2H_4 reduction, Angew. Chem. 126 10653 10657.

[8] Chen D., Liu C., Chen S., Shen W., Luo X., Guo L., (2016). Controlled synthesis of recyclable, porous FMO/C@TiO_2 core-shell nanofibers with high adsorption and photocatalysis properties for the efficient treatment of dye wastewater, ChemPlusChem 81 282–291.

[9] Chen D., Huang Z., Quan H., Chen S., Lin J., Luo X., Guo L., (2016). Mesoporous single crystal rutile TiO_2 rods modified with Ag nanoparticles as a photocatalyst for degradation of pollutants, Sci. Adv. Mater. 4 760–766.

[10] Ida S., Yamada K., Matsunaga T., Hagiwara H., Matsumoto Y., Ishihara T., (2010). Preparation of p-type $CaFe_2O_4$ photocathodes for producing hydrogen from water, J. Am. Chem. Soc. 132 17343–17345.

[11] Iwashina K., Kudo A., (2011) Rh-Doped $SrTiO_3$ Photocatalyst electrode showing cathodic photocurrent for water splitting under visible light irradiation, J. Am. Chem. Soc. 13 13272–13275.
[12] Zhao W., Jin Y., Gao C.H., Gu W., Jin Z.M., Lei Y.L., Liao L.S., (2014). A simple method for fabricating pen junction photocatalyst $CuFe_2O_4/Bi_4Ti_3O_{12}$and its Photocatalytic activity, Mater. Chem. Phys. 143 952–962.
[13] Yu Q., Meng X.G., Wang T., Li P., Liu L.Q., Chang K., Liu G.L., Ye J.H., (2014). A highly durable p-$LaFeO_3$/n-Fe_2O_3 photocell for effective water splitting under visible light, Mater. Chem. Phys. 143 952–962.
[14] Wu Y., Chen D.Z., Quan H.Y., Wu S.L., Luo X.B., Guo L., (2016). Enhanced Photocatalytic properties of ZnFe2O4-doped $ZnIn_2S_4$ heterostructure under visible light irradiation, RSC Adv. 6 83012–83019.
[15] Yong X., Martin A.A. Schoonen, (2000). The absolute energy positions of conduction and valence bands of selected semiconducting minerals, Am. Mineral. 85 543–556.
[16] Kudo A., Miseki Y., (2009). Heterogeneous photocatalyst materials for water splitting, Chem. Soc. Rev. 38 253–278.
[17] Jiang X., Lin Q., Zhang M., He G., Sun Z., (2015). Microstructure, optical properties, and catalytic performance of Cu_2O-modified ZnO nanorods prepared by electrodeposition, Nanoscale Res. Lett. 10 1–6.
[18] Deo M., Shinde D., Yengantiwar A., Jog J., Hannoyer B., Sauvage X., More M., Ogale S., (2012). Cu_2O/ZnO hetero-nanobrush: hierarchical assembly, field emission and photocatalytic properties, J. Mater. Chem. 22 17055–17062.
[19] Hameş Y., Eren San S., (2004). CdO/Cu_2O solar cells by chemical deposition, Sol. Energy 77 291–294.
[20] Yang L.X., Luo S.L., Li Y., Xiao Y., Kang Q., Cai Q.Y., (2010). High efficient Photocatalytic degradation of p-nitrophenol on a unique Cu2O/TiO2 p-n heterojunction network catalyst, Environ. Sci. Technol. 44 7641–7646.
[21] Kim T.W., Ha H.W., Paek M.J., Hyun S.H., Choy J.H., Hwang S.J., (2010). Unique phase transformation behavior and visible light photocatalytic activity of titanium oxide hybridized with copper oxide, J. Mater. Chem. 20 3238–3245.
[22] Jiang T.F., Xie T.F., Yang W.S., Chen L.P., Fan H.M., Wang D.J., (2013). Photoelectrochemical and photovoltaic properties of p-nCu_2O homojunction films and their photocatalytic performance, J. Phys. Chem. C 117 4619–4624.
[23] Wang P., Wu H., Tang Y.M., Amal R., Ng Y.H., (2015).Electrodeposited Cu_2O as photoelectrodes with controllable conductivity type for solar energy conversion, J. Phys. Chem. C 119 26275–26282.
[24] Pan A.A., Tamirat C., Chen A.G., Su H., Chen W., Rick C., Ayele J., Aragaw D.W., Lee B.A., Yang J., Hwang Y, B., (2015). Heterostructured Cu_2O/CuO decorated with nickel as a highly efficient photocathode for photoelectrochemical water reduction, J. Mater. Chem. A 23 12482–12499.
[25] Yong X., Martin A.A. Schoonen, (2000). The absolute energy positions of conduction and valence bands of selected semiconducting minerals, Am. Mineral. 85 543–556.
[26] Kudo A., Miseki Y., (2009). Heterogeneous photocatalyst materials for water splitting, Chem. Soc. Rev. 38 253 –278.
[27] Wang P., Wen X., Amal R., Y.H. Ng, (2015). Solar hydrogen generation from seawater with a modified BiVO4 photoanode, RSC Adv. 5 5231–5236.
[28] Zhang Z.H., P. Wang, Highly stable copper oxide composite as an effective photocathode for water splitting via a facile electrochemical synthesis strategy, J. Mater. Chem. 22 (2012) 2456–2464.
[29] Kargar A., Partokia S.S., Niu M.T., Allameh P., Yang M., May S., Cheung J.S., Sun K., Xu K., Wang D., (2014). Solution-grown 3D Cu_2O networks for efficient solar water splitting, Nanotechnology 25 (20) 205401.
[30] Mahmoud M.A., Qian W., El-Sayed M.A., (2011). Following charge separation on the nanoscale in Cu_2O-Au nanoframe hollow nanoparticles, Nano Lett. 11 (8) 3285-3289.
[31] Zhang Z., Wang P., (2012). Highly stable copper oxide composite as an effective photocathode for water splitting via a facile electrochemical synthesis strategy, J. Mater. Chem. 22 (6) 2456-2464.
[32] Paracchino A., Laporte V., Sivula K., Gratzel M., Thimsen E., (2011) Highly active oxide photocathode for photoelectrochemical water reduction, Nat. Mater. 10 (6) 456-461.

[33] M. Abdurrahman, F.W Burari, & O.W Olasoji**.** Facile Fabrication of MoS_2/ZnO Hetero-Epitaxial Growth on Cu_2O with Enhanced Photoelectrochemical Activity Through Thermal Oxidation Process. Algerian Journal of Renewable Energy and Sustainable Development. Volume: 5| Number: 2 | 2023| December. 5(2) 2023: 117-126, doi: 10.46657/ajresd.2023.5.2.3

[34] M. Abdurrahman, F.W. Burari, Maje Alhaji Haruna, Aminu I., Abdullahi T., O.W. Olasoji, Shehu M., H.Y. Shuaibu, M.T. Garba, J. Mohammed**.** An affordable fabrication and synthesis of novel Bi/Cu_2O/Bi hetero-structure pec solar cell. Science World Journal Vol. 18(No 1) 2023. 1*597-6343 (Online), ISSN: 2756-391X*

[35] M. Abdurrahman, F.W Burari, & O.W Olasoji. Photoelectrochemical solar cells enactment of ternary MoS_2/WS_2/Cu_2O based photocathode under visible-light irradiation. Arabian Journal of Chemical and Environmental Research. Vol. 09 Issue 01 (2022) 218–231

[36] M. Abdurrahman, F.W Burari, & O.W Olasoji. Photo electrochemically Manufactured HgO/Cu_2O Monolayer with Augmented Photovoltaic Features. Computational and Experimental Research in Materials and Renewable Energy (CERiMRE) Volume 5, Issue 2, page 142-151